Preparation and Electrorheological Characterization of Suspensions of Poly(urethane acrylate)/Clay Nanocomposite Particles

Jung-Bae Jun, Kyung-Do Suh

Division of Chemical Engineering, College of Engineering, Hanyang University, Seoul 133-791, South Korea

Received 16 July 2002; accepted 23 January 2003

ABSTRACT: Micron-sized poly(urethane acrylate) (PUA)/clay nanocomposite particles were synthesized by suspension polymerization. UA containing a poly(ethylene oxide) group in the main chain was first inserted into the silicate layers of montmorillonite clay through mixing the UA with the clay. Then, ethylene glycol dimethacrylate and an oil-soluble initiator were added into this UA/clay mixture, followed by the emulsification of the monomer mixture in an aqueous solution of polymeric stabilizer. Suspension polymerization was carried out at 60°C for 12 h to obtain the PUA/clay composite particles. The incorporation of clay into the polymer phase was verified by FTIR spectroscopy, and the intercalation structure of the clay composite was confirmed by X-ray diffraction analysis. Other characterizations including thermal analysis, morphological observation, and dielectric analysis were also performed. After suspensions of bare PUA and PUA/clay nanocomposite particles in silicone oil were prepared, their electrorheological properties were measured under various electric fields and compared. © 2003 Wiley Periodicals, Inc. J Appl Polym Sci 90: 458–464, 2003

Key words: electrorheology; clay nanocomposites; urethane acrylate; suspension polymerization

INTRODUCTION

The electrorheological (ER) effect of fluids, which was first reported by Winslow[1] in 1949, has been extensively studied for the last two decades and reviewed in several publications.[2–6] ER fluids are generally composed of polarizable solid particles suspended in an insulating oil. They are typically fluids in the absence of an electric field; however, the fluids can solidify into viscoelastic solids in milliseconds under a large external electric field. This behavior is attributed to the structural change of suspended particles by the applied electric field. When electric fields are applied to the fluids, field-induced dipoles of suspended particles attract each other and cause the particles to form chains or fibrillated structures in the direction of the field. These chains inhibit the fluid flow and consequently increase the apparent viscosity and shear yield stress of fluids. On the other hand, the rheological properties of the fluids recover the original state promptly when the applied field is removed. This fast, strong, and reversible change in rheological properties provides novel and efficient approaches for energy transfer and motion control in devices such as clutches, dampers, brakes, valves, or actuators.[4,7,8] However, despite the great potential of ER technology, few versatile ER devices have reached the marketplace due to a lack of effective fluids.

In order to acquire a high ER performance for a specific application, the fluids should satisfy several requirements: a high dynamic yield stress, a dramatic increase in the apparent viscosity, stability against sedimentation, a low current density, fast response times, and so on.[8] These properties are preferentially determined by the characteristics of the two components of ER fluid, the dispersed particle phase and the suspending medium oil, and the interfacial properties. In addition, most ER suspensions contain additives such as surfactants and activators to enhance ER activity and to improve colloidal stability of the dispersed particles.[9–11] Recent patents[12,13] and studies[11,14–17] revealed the complexing of different materials, such as organic with inorganic, to obtain superior ER materials. Li et al.[14] disclosed that the ER effects of γ-Fe_2O_3/lithium polyacrylate composite particles at some γ-Fe_2O_3 contents are stronger than that of lithium polyacrylate, especially under alternating fields. Clay minerals have been introduced into the ER materials as nanocomposites with organic polymers including styrene-acrylonitrile copolymer[15] and polyaniline.[16] Park et al.[17] reported an interesting result that the polyaniline-coated clay nanocomposite particles strongly induced the formation of a particle network structure, causing a dramatic enhancement of yield stress. Therefore, composite particles are often

Correspondence to: Prof. K.-D. Suh (kdsuh@hanyang.ac.kr).
Contract grant sponsor: Brain Korea 21 Project.

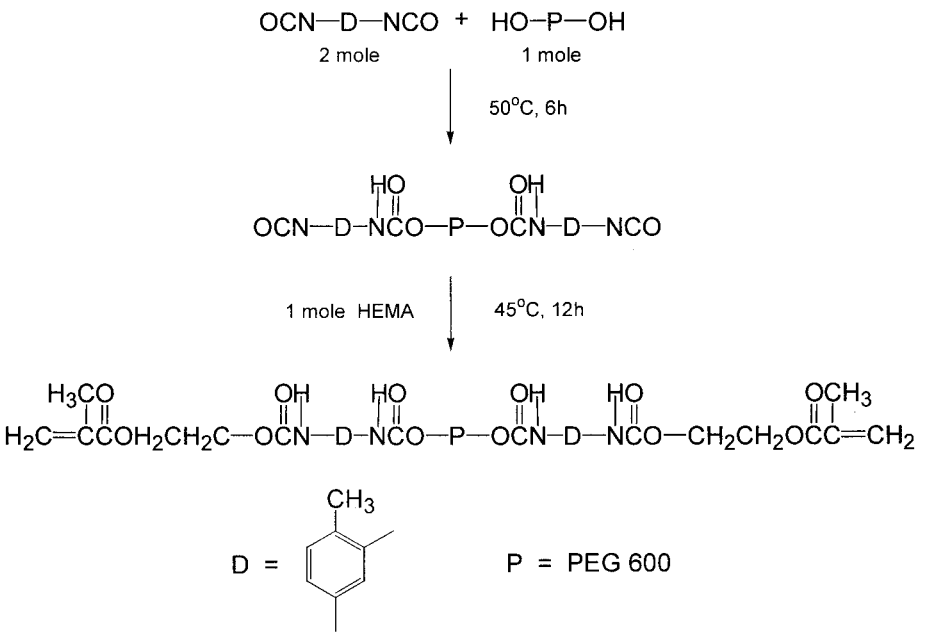

Scheme 1 The reaction procedure and the molecular structure of the UA synthesized in the study.

preferred to obtain superior ER properties by regulating the particle characteristics including the particle dielectric properties, constitution of the surface, the density, and so forth.

In this study, we synthesized polymer/clay nanocomposite particles by using suspension polymerization of monomer-intercalated clay mixtures and used them as an ER material. The influence of clay incorporation both on the particle characteristics, such as morphological, thermal and dielectric properties, and on the ER activity was investigated.

EXPERIMENTAL

Materials

Toluene diisocyanate (TDI, 80% 2,4-isomer, Tyoko Chemical Industry Co.) was vacuum distilled before use. Polyethylene glycol (PEG, M_w = 1000 g mol^{-1}, Aldrich Chemical) and poly(vinyl alcohol) [PVA, M_w = (8.8–9.2) × 10^4 g mol^{-1}, 87–89% hydrolyzed, Kuraray Co.] were used as received. The inhibitors in 2-hydroxyethyl methacrylate (HEMA, Aldrich) and ethylene glycol dimethacrylate (EGDMA, Tyoko Chemical Industry Co.) were removed through a removing column (Aldrich). 2,2′-Azobis(dimethyl valeronitrile) (ADVN, Wako Chemical) was used as the radical initiator and recrystallized from methanol before use. The clay purchased from Southern Clay Products was a natural montmorillonite (MMT, Cloisite 25A) modified with a quaternary ammonium salt.

Synthesis of urethane acrylate (UA)

The synthesis of UA followed our previous experiments.[18,19] All reactions were carried out in a four-necked glass reactor equipped with a stirrer, a reflux condenser, thermocouples, and a nitrogen inlet system. TDI (2 mol) was reacted with 1 mol PEG at 50°C for 6 h, producing a molecular structure having a PEG chain in the middle and isocyanates at the ends. After dissolving 1 wt % dibutyltinlaurate in the reactor, 2 mol HEMA was reacted with the residual isocyanate groups at 45°C for 12 h, which capped the molecular ends with reactive vinyl groups. The reaction procedure and the molecular structure of the UA synthesized are presented in Scheme 1.

Particle preparation by suspension polymerization

The suspension polymerization reaction was performed in a 500-mL round-bottomed glass flask. The continuous phase comprised 270 g of an aqueous solution of PVA (0.5% w/w) and sodium nitrite (0.01% w/w). The dispersed phase comprised 24 g of monomer (UA plus EGDMA in a weight ratio of 6:4), 6 g of toluene as an organic diluent, and the oil-soluble initiator ADVN (1 wt % vs. total monomer weight).

In the case of clay incorporation, the UA was first mixed with MMT clay (5 wt % vs. total monomer weight) for 2 h by using a high-speed mechanical stirrer. Then, EGDMA, toluene, and initiator were added and well mixed at room temperature for 1 h. Emulsification was achieved by shearing the monomer/clay mixture and an aqueous phase under an atmosphere of nitrogen for 10 min. Agitation was provided by a homomixer rotating at 1000 rpm. Polymerization was carried out at 60°C for 12 h using a thermostatted water bath at a reduced stirrer speed of 300 rpm. The resulting polymer particles were centrifuged for 10 min at 3000 rpm. The supernatant was

TABLE I
Standard Recipe for Suspension Polymerization

	Ingredient	PUA (g)	PUA/Clay (g)
Oil phase	Urethane acrylate	14.4	13.68
	MMT clay	0	1.2
	EGDMA	9.6	9.12
	Toluene	6	6
	ADVN[a]	0.24	0.228
Aqueous phase	Water	267	267
	Poly(vinyl alcohol)	3	3

The conditions were a temperature of 60°C for 12 h with a 10 wt % monomer phase concentration based on the total weight.

[a] 1.0 wt % ADVN based on the total monomer weight.

then decanted and the remaining precipitate was repeatedly washed by three centrifugation/redispersion processes in ethanol and dried under a vacuum at 80°C overnight. All the ingredients are summarized in Table I.

Characterizations

The complexing of clay with the polymeric phase was identified by FTIR analysis. X-ray scattering experiments were conducted with a Rigaku D/Max-2200 (copper radiation, 40 kV, 100 mA, nickel filter) in the range of 2θ = 2–10°. To study the thermal stability of the particles, thermogravimetric analysis (TGA) was carried out in the temperature range of 30–600°C at a heating rate of 20°C/min under a nitrogen atmosphere on a SDT2960 (TA Instrument, Inc.). The particle morphology was observed with a scanning electron microscope (JSM-6330F, Jeol), and the particle size was measured by a Coulter counter (Multisizer II, Coulter Co.). The dielectric properties of the pelletized particles were measured in a frequency range of 10^0–10^5 Hz with a dielectric spectrometer (Concept 40, Novocontrol).

Then, ER suspensions were prepared by dispersing the particles in silicone oil (KF-96, 50 cS, Shinetsu) at a particle weight fraction of 20% using mechanical stirring (1500–2000 rpm). The rheological properties of the ER suspensions were measured using a rotational rheometer (ARES4, Rheometric Scientific Co.) equipped with a low-range transducer, Couette geometry, and a high-voltage power generator (model EL5P8L, Glassman Co.). The ER fluids were placed in the gap between the rotating outer cup and the stationary inner bob. An electric field was applied for 5 min in order to obtain an equilibrium structure before applying the shear. The shear rate was varied from 10^{-1} to 10^3 s^{-1} and the flow curves were obtained with the rheometer operating in the controlled shear rate (CSR) mode. Electric current going through the ER fluid was measured at a quiescent state using a Keithley 196 system.

RESULTS AND DISCUSSION

The structure of the composite particles was analyzed by using FTIR spectroscopy and X-ray diffraction (XRD) analysis. Figure 1 shows the FTIR spectra for pristine clay, highly crosslinked poly(UA) (PUA), and PUA/clay composite particles. The pure MMT clay showed three strong peaks at 455, 520, and 1,045 cm^{-1}. These peaks are associated with the bending mode of Si—O, the stretching vibration of Al—O, and the stretching vibration of Si—O, respectively. The organic PUA component showed a characteristic band at 1730 cm^{-1}, which is associated with the C═O stretching of acrylates. One can easily find strong characteristic peaks of both the clay and the PUA component in the spectrum of PUA/clay composite particles. Thus, it is thought that the *in situ* suspension polymerization of the monomer/clay mixture can successfully produce clay-incorporated polymer particles.

Figure 2 shows the XRD patterns for PUA/clay composite particles and pure clay. The organomodified MMT clay showed a characteristic peak at 2θ = 4.85°, giving the silicate–interlayer spacing value of 18.2 Å. However, this strong peak nearly disappeared in the PUA/clay composite particles, indicating that the silicate layer of the MMT clay was intercalated and/or partially exfoliated by the insertion of poly(ethylene oxide)-containing chains through mixing of the MMT clay with UA as a bulk state. It is well known that poly(ethylene oxide) can intercalate into layered silicates to form nanocomposite materials.[20,21]

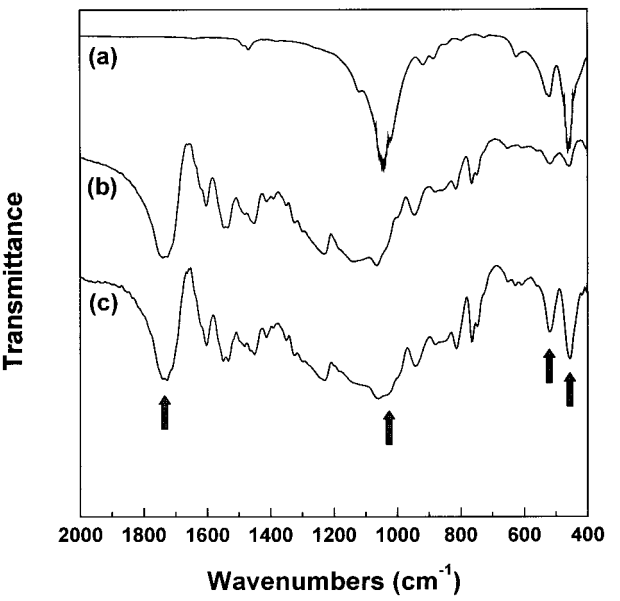

Figure 1 FTIR spectra of (a) pristine MMT clay, (b) bare PUA particles, and (c) PUA/clay composite particles.

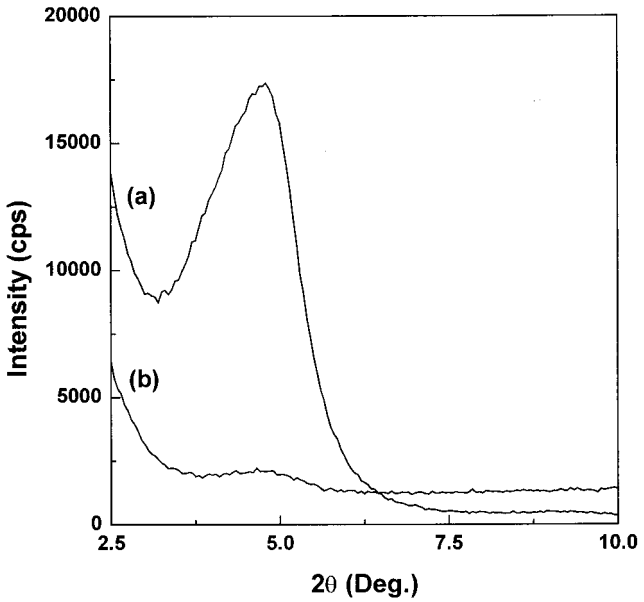

Figure 2 The X-ray diffraction angle patterns of (a) MMT clay and (b) PUA/clay composite particles.

From the results, it appears that the MMT clays exist in the composite particles as separate nanoscale plates within the polymer chains, and consequently the synthesized PUA/clay can be termed nanocomposite particles.

Scanning electron photographs of the PUA particles and PUA/clay nanocomposite particles are shown in Figure 3. Although all the particles are round, the particle surfaces are coarsely rough and raspberry-like. This uneven surface might be due to the high viscosity and the high degree of crosslinking of the dispersed droplet phase during the suspension polymerization. However, the polymerization system was very stable and there was no macroscopic aggregation. All the particles ranged in size range from ~5 to 100 μm. The average diameters of the PUA particles and the PUA/clay composite particles were 45.6 and 55.1 μm, respectively. This difference in size is because the apparent viscosity of the monomer mixture is increased by the addition of clay. That is, high-viscosity monomer droplets deform less and break up to generate larger droplets compared to low-viscosity droplets under the same shearing conditions. However, the two series of particles are fairly adequate in size for use in ER fluids and the effect of the size difference between the two series on the ER properties is quite negligible.

Figure 4 shows the TGA thermograms for pure PUA particles and the PUA/clay composite particles. Both particles showed no weight loss under 270°C and decomposition of the particles commenced at around 300°C. This result shows that the highly crosslinked PUA-based particles are completely anhydrous and possess relatively good thermal stability. Moreover, it was found that the PUA/clay nanocomposite particle exhibited a slightly higher thermal decomposition temperature compared to pure PUA particles. The thermal decomposition temperatures of the PUA and PUA/clay composite particles were 432.7 and 437.5°C, respectively. The PUA/clay composite particles left a residue of about 6.4% at 600°C, whereas the PUA particles left a residue of about 2.4% at the same temperature. From this result, it is calculated that over 80% of the initial clay added was quantitatively introduced into the particles.

Based on the dielectric polarization[5,22] of ER fluids arising from the difference between the dielectric constants of the dispersed particles and the medium oil, it can be simply thought that particulate materials of higher dielectric constant, except barium titanate,[23] are advantageous for superior ER effects. Figure 5 shows the variation of the dielectric constants as a function of the applied electrical frequency for the

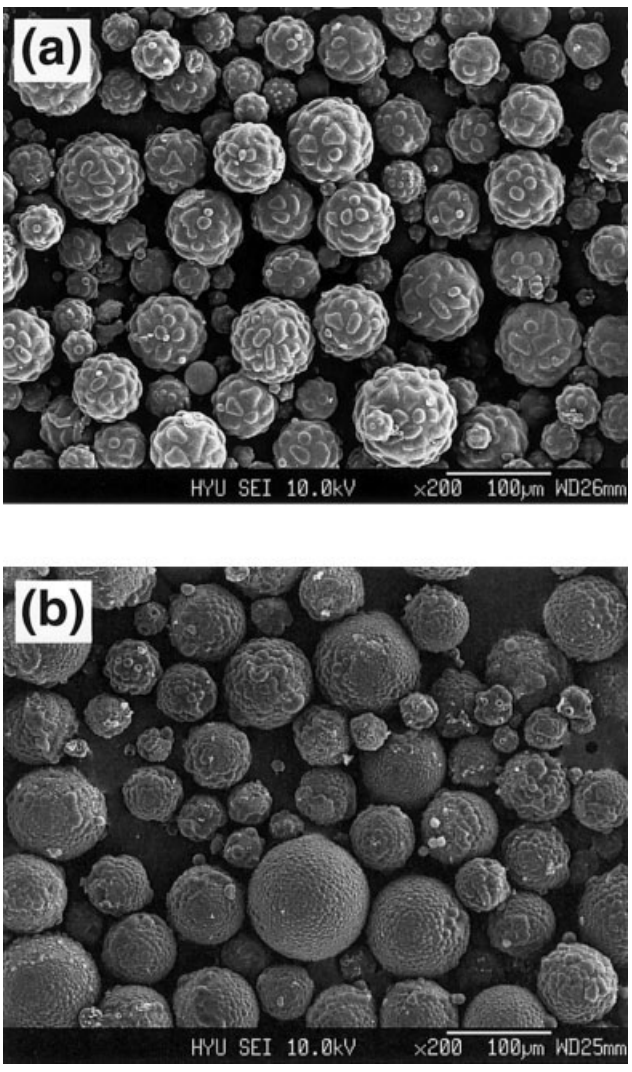

Figure 3 Scanning electron micrographs of (a) bare PUA particles and (b) PUA/clay composite particles.

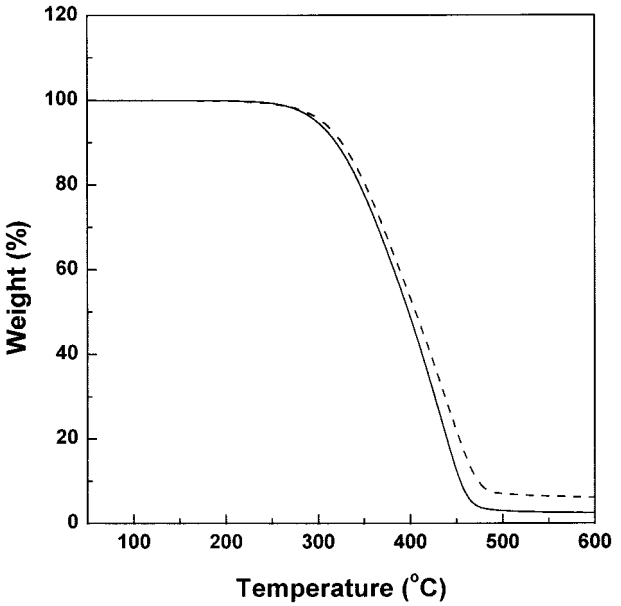

Figure 4 (—) TGA thermograms of bare PUA particles and (- - -) PUA/clay composite particles.

PUA and PUA/clay composite particles. The clay-incorporated PUA particles exhibited significantly increased dielectric constant values over the bare PUA particles. The increase in the dielectric constant of clay nanocomposite particles would result in an enhancement of the ER effect by increasing the particle polarizability (β)[3,5] which is defined as

$$\beta = [\varepsilon_p - \varepsilon_o]/[\varepsilon_p + 2\varepsilon_o]$$

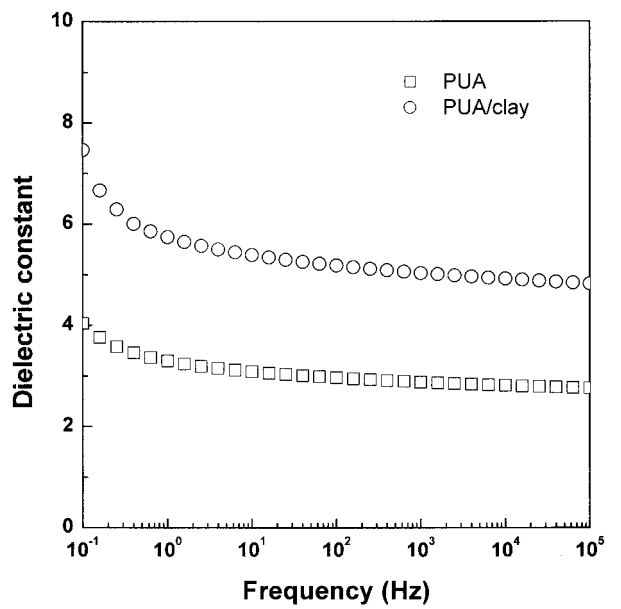

Figure 5 The dielectric constants as a function of the applied electrical frequency for bare PUA and PUA/clay composite particles.

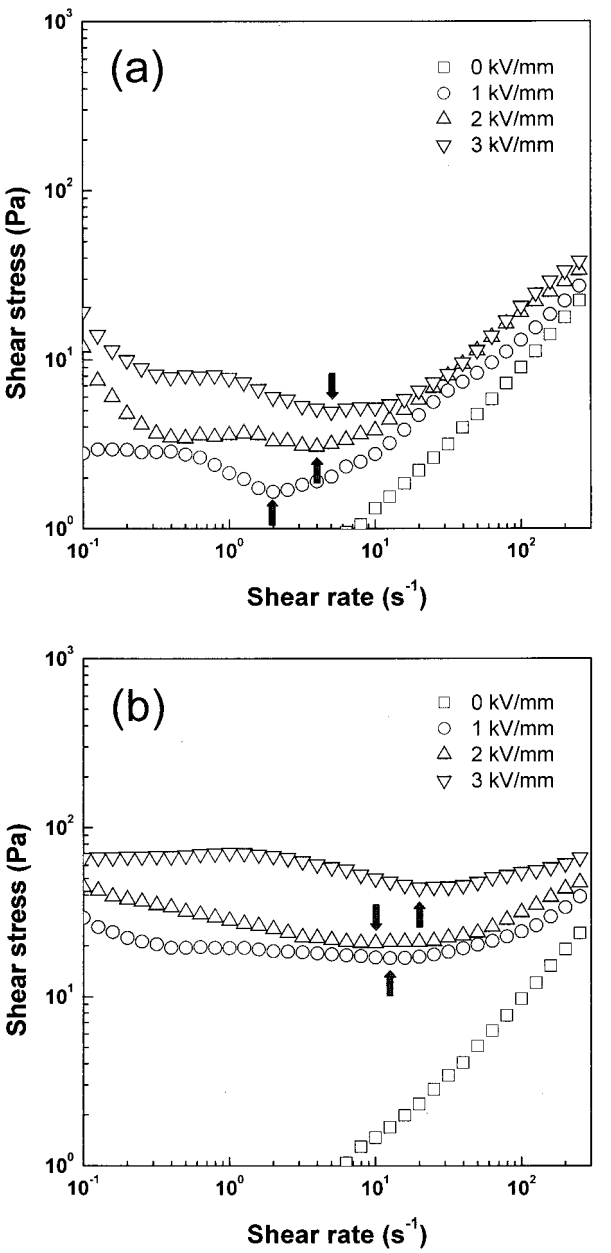

Figure 6 The flow curves of the shear stress versus the shear rate for 20 wt % suspensions of (a) bare PUA and (b) PUA/clay composite particles at different electric fields.

where ϵ_p is the dielectric constant of the particulate phase and ϵ_o is that of the oil phase. In this study, because the oil phase is fixed, only the dielectric property of the particulate phase can alter the particle polarizability.

The flow curves of the shear stress (τ) versus the shear rate (γ) from the CSR experiment for the ER suspensions at various electric field strengths are illustrated in Figure 6. In the absence of an electric field, the shear stress increased linearly with the shear rate, behaving like a Newtonian fluid. However, similar to most ER fluids, PUA-based ER fluids showed highly increased shear stresses in the presence of electric

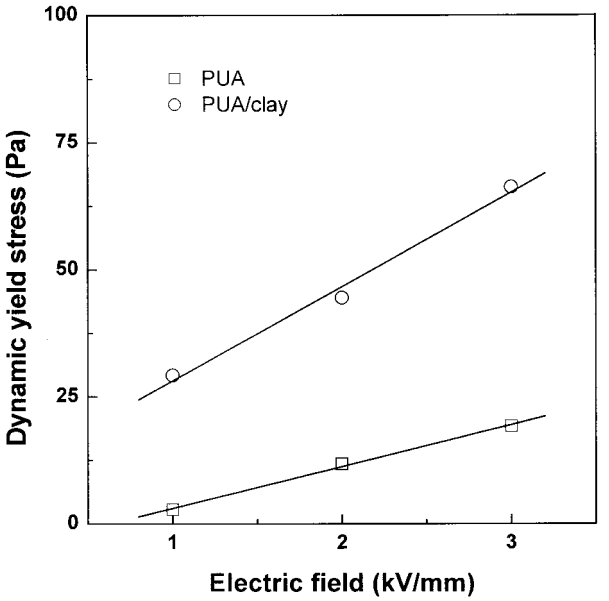

Figure 7 The dynamic yield stresses as a function of the applied electric field for 20 wt % suspensions of two PUA-based particles.

fields, displaying yield stresses. Bare PUA suspensions showed relatively low shear stress under the electric fields; on the other hand, the suspension of PUA/clay composite particles gave much-enhanced shear stresses at the same electric field. For both of the ER fluids, as the shear rate increased, the shear stress decreased until a critical shear rate (arrow, Fig. 6), showing a minimum shear stress, then increased with the shear rate. At lower shear rates than the critical shear rates, the fibrillated structures of the suspending particles started to deform at the initial stage and the structures were consequently destroyed, resulting in a gradual decrease in the shear stress. However, the shear stress increased again above the critical shear rates. In this high-shear region, the stress behavior of the fluids is thought to be largely dominated by the hydrodynamic force generated by shear and the ER fluid exhibits a linear relationship between the shear stress and the shear rate, behaving like a pseudo-Newtonian fluid. One can also easily find that the critical shear rate depends on the applied electric field strength, increasing with the field strength. Note that compared to the bare PUA suspension, the PUA/clay nanocomposite suspension did not show serious decreases in shear stresses over the applied shear rates.

Dynamic yield stresses can be obtained by extrapolating the shear rate to zero under a CSR test. In this study, the stress at the lowest shear rate ($\gamma = 0.1\ s^{-1}$) was regarded as the dynamic yield stress. Figure 7 shows the dynamic yield stress for the two ER fluids as a function of the electric field strength. The bare PUA suspension showed very low yield stresses under electric fields, whereas the clay-incorporated PUA suspension exhibited relatively higher yield stresses and the magnitude increased with the increase of the electric fields. The yield stresses of the PUA/clay suspension were over three times larger than those of the bare PUA suspension under all electric field strengths. It seems that the clay incorporated in the PUA particles largely affects the particle dielectric properties and thus induces the dipole formation to be facilitated and strong.

Figure 8 shows the current density of the bare PUA and the PUA/clay composite suspensions as a function of the applied electric field strength. The suspensions showed relatively low current densities over the applied electric fields, and the current density was moderately increased with the field strength. It is noted that the current densities of the PUA/clay composite suspension are higher than those of the bare PUA suspension. However, the current density of our ER fluids is much less than the commercial requirement (~30 $\mu A/cm^2$ at 6 kV/mm), exhibiting better electrical stability.

CONCLUSIONS

Micron-sized PUA-based polymer particles and the corresponding clay composite particles were successfully synthesized by suspension polymerization of a UA/EGDMA/clay mixture. The synthesis of PUA/clay composite particles was confirmed by IR spectra and XRD patterns, and the clay was found to exist as a PUA-intercalated structure in the composite particles. The PUA-based particles had relatively good thermal stability, and the clay introduction somewhat

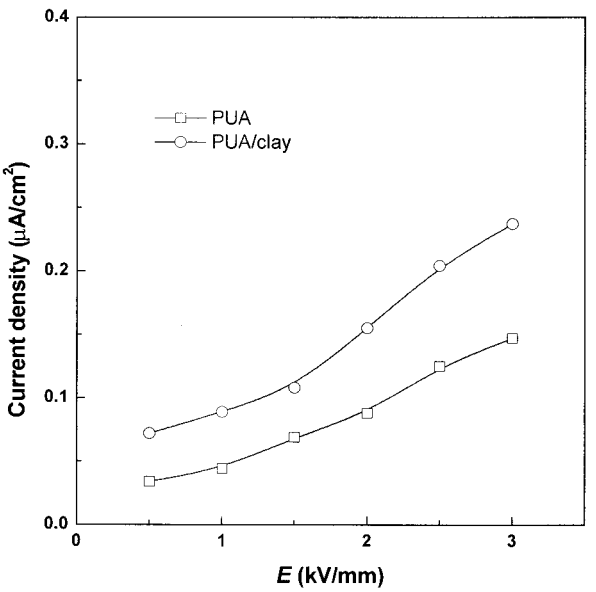

Figure 8 The current density of the bare PUA suspension and the PUA/clay composite suspension as a function of the electric field strength (E).

enhanced the thermal decomposition temperature. All the particles were completely anhydrous and morphologically spherical, ranging in size from ~5 to 100 μm. The clay incorporated in the PUA particles also increased the particle dielectric constant and consequently increased the ER properties. The suspension of PUA/clay nanocomposite particles exhibited much higher yield stresses compared to the suspension of bare PUA particles over all the electric fields. This enhancement in the ER effect is attributed to the clay phase that is well dispersed in the polymer particles, inducing the permittivity increase and hence the particle polarizability increase as well.

This work was supported by the Engineering Research Center (ERC) for Advanced Functional Polymers of Korea.

References

1. Winslow, W. M. J Appl Phys 1949, 20, 1137.
2. Block, H.; Kelly, J. P. J Phys D Appl Phys 1988, 21, 1661.
3. Gast, A. P.; Zukoski, C. F. Adv Colloid Interface Sci 1989, 30, 153.
4. Burchill, P. J. Mater Forum 1991, 15, 197.
5. Parthasarathy, M.; Klingenberg, D. J. Mater Sci Eng 1996, 17, 57.
6. Hao, T. Adv Colloid Interface Sci 2002, 97, 1.
7. Shylman, Z. P.; Gorodkin, R. G.; Korobko, E. V.; Gleb, V. K. J Non-Newton Fluid Mech 1981, 8, 29.
8. Habelka, K. O.; Pialet, J. W. CHEMTECH 1996, 26, 36.
9. Kim, Y. D.; Klingenberg, D. J. J Colloid Interface Sci 1996, 183, 568.
10. Lee, H. J.; Chin, B. D.; Yang, S. M.; Park, O. O. J Colloid Interface Sci 1998, 206, 424.
11. Dürrschmidt, T.; Hoffmann, H. Colloid Surface A 1999, 156, 257.
12. Edamura, K.; Otsubo, Y.; Mizoguchi, M. U.S. Pat. 5,695,678, 1997.
13. Fujita, T.; Kondo, T.; Saiki, H. Jpn. Pat. 08-012,987, 1996.
14. Li, X.; Zhang, L.; Ji, R. Polym Adv Technol 1999, 10, 90.
15. Kim, J. W.; Choi, H. J.; John, M. S. Macromol Symp 2000, 155, 229.
16. Kim, J. W.; Kim, S. G.; Choi, H. J.; John, M. S. Macromol Rapid Commun 1999, 20, 450.
17. Park, J. H.; Lim, Y. T.; Park, O. O. Macromol Rapid Commun 2001, 22, 616.
18. Kim, J. Y.; Suh, K. D. Macromol Chem Phys 1996, 197, 2429.
19. Kim, J. W.; Suh, K. D. Colloid Polym Sci 1999, 277, 210.
20. Vaia, R. A.; Vasudevan, S.; Krawiec, W.; Scanlon, L. G.; Giannelis, E. P. Adv Mater 1995, 7, 154.
21. Vaia, R.; Sauer, B. B.; Tse, O. K.; Diannelis, E. P. J Polym Sci Polym Phys 1997, 35, 59.
22. Davis, L. C. J Appl Phys 1992, 72, 1334.
23. Hao, T.; Kawai, A.; Ikazaki, F. Langmuir 1998, 14, 1256.